MODELING Ka BAND SCINTILLATION AS A FRACTAL PROCESS

Nedo Celandroni, *Member*, *IEEE* and Francesco Potortì

CNUCE, Institute of CNR (Italian National Research Council)
Via S. Maria 36 - 56126 Pisa - Italy
Phone: +39-50-593207/593203
Fax: +39-50-904052 - Telex: 500371
E-mail: N.Celandroni@cnuce.cnr.it, F.Potorti@cnuce.cnr.it

Key words: scintillation, rain fade, fractal model, signal degradation, fade countermeasures.

Abstract

We propose a model that describes the signal fading process due to scintillation in the presence of rain. We analyzed a data set of up-link (30 GHz) and down-link (20 GHz) attenuation values averaged over 1 second intervals. The data are samples relative to 10 significant events, for a total of 180,000 s, recorded at the Spino d'Adda (North of Italy) station using the Olympus satellite.

Our analysis is based on the fact that the plot of attenuation versus time recalls the behaviour of a self-similar process. We then make various considerations and propose a fractional Brownian motion model for the scintillation process. We describe the model in detail, with pictures showing the apparent self-similarity of the measured data. We then show that the Hurst parameter of the process is a simple function of the rain fade.

We describe a method for producing random data that interpolate the measured samples, while preserving some of their interesting statistical properties. This method can be used for simulating fade countermeasure systems.

As a possible application of the model, we show how to optimise fade measurement times for fade countermeasure systems.

Preprint of an article published on the IEEE JOURNAL on SELECTED AREAS in COMMUNICATIONS, VOL. 17, No. 2
Copyright 1999 by IEEE. <URL: http://www.ieee.org/>

1. Introduction

Using the Ka band entails dealing with signal attenuation due to rain and scintillation, since the amplitude of both these phenomena increases with frequency [11, 12]. Fade countermeasure systems, such as transmission power [9], bit and coding rates adaptation [1, 2], frequency [12, 13] or space diversity [10] are thus required to avoid loss of economy.

All these systems need a quick and accurate measurement of link degradation, due to atmospheric events, in order to reduce the power margins over the countermeasure's thresholds of intervention.

The estimation accuracy of both the attenuation and the signal to noise ratio is generally inversely proportional to the measurement time. Furthermore, due to the satellite transmission delay and the algorithm used, there is an interval of time, in the order of one or two seconds, between the countermeasure application and the actual reception of data by the destination user. By observing a selected sample of experimental attenuation data we revealed that linear regression methods were not useful for short term predictions of attenuation, an opinion which is also shared in [5]. The short time attenuation fluctuations (expressed in dB), in fact, seem to have a Gaussian distribution and a small autocorrelation. This phenomenon is mostly attributed to scintillation, i.e. signal amplitude variations due to tropospheric turbulence [20], rather than to raindrop absorption and scattering. Scintillation occurs both during periods without attenuation (*dry scintillation*) and also during rain (*wet scintillation*) [28]. Instead of trying to predict the attenuation value, our approach is to estimate the variance of its evolution. Then, in order to compensate for attenuation evolution and measurement inaccuracy, we can introduce a suitable power margin. This paper presents a fractal model of the attenuation behaviour that is applicable for time intervals of a few seconds. As examples of possible applications, we show how to generate synthetic attenuation data for simulating fade countermeasure systems, and we describe a procedure for optimising both the attenuation measurement time and the power margin needed.

In Section 2 we mention how we first thought about using a fractal model for our set of attenuation measurements. We continue in Section 3 with an overview of fractional Brownian motion, then in Section 4 we describe our model. In Section 5 we suggest some possible links between the parameters we found by geometrical means and experimental findings on scintillation processes which are found in the literature. Sections 6 and 7 give an outline of possible applications.

Preprint of an article published on the IEEE JOURNAL on SELECTED AREAS in COMMUNICATIONS, VOL. 17, No. 2

2. Interpolation of a set of measured attenuation values

Our experimental traces of the signal power attenuation are available as averages over one-second time intervals, a time resolution which is about four times the round trip time of a geostationary satellite and is typical of this kind of measurement. As we noted above, fade countermeasure systems require a quick and accurate measurement of the attenuation value, and this estimate must be disseminated as soon as possible so that the satellite network can apply the adaptive countermeasure.

One approach to simulating rain fade events could be to take a rain attenuation trace and interpolate it, in order to synthetically compute attenuation samples at a higher rate than the measurement rate.

The traces highlight that any kind of elementary interpolation method would lead to the process behaving unrealistically. Linear or spline interpolation, for example, would create at small scales (i.e. between measured samples) a smooth graphic that is by no means similar to what is observed at coarser scales. This discrepancy is important for the problem at hand, because we need to check the behaviour of the prediction algorithms when the samples are noisy. We therefore propose a different approach, which was inspired by the apparent statistical self-affinity of the measured power attenuation. In Figure 4, the same rain event is magnified and suitably rescaled. One can see what appears to be the footprint of a rescaled self affine random process: without the help of the numbers on the horizontal axis, it would be difficult to tell whether any one picture is taken on a greater or smaller scale than the others.

While interpolation analyses are commonly carried out by using elementary functions, which are derivable and hence smoothed at a small enough scale, in most cases this approach is only dictated by simplicity issues, and by the use of a common language of science. In the last few decades the concept of fractal geometry has emerged as a paradigm that gives scientists a new common language, which is useful for dealing with natural phenomena that cannot be approximated by elementary functions without losing their meaning [19].

By using a fractal language we manage, in a natural way, to account for the oscillating behaviour of the attenuation traces, which is the most important feature a measurement and prediction system has to deal with.

3. Fractional Brownian motion and statistical self-affinity

A stochastic process A(t) is said to be statistically self-affine if, for any given positive real number r, its statistics are the same as those of the process $kA(t/r)$, where k depends on r.

One such process is Brownian Gaussian motion, that is, a process with stationary independent Gaussian increments.

Let us denote this process by *B*. If we consider discrete times t_i, $B_{i+1} - B_i$ is, by definition, a Gaussian random variable with null mean and variance σ^2. The increment $B_{i+1} - B_i$ is stationary, that is, it does not depend on the index *i*. Moreover, it is independent of other increments as well, that is, the increments $B_{i+1} - B_i$ are i.i.d. variables. Given these properties, the increment process $W(i, j) = B_i - B_j$ is only dependent on the difference $k = i\text{-}j$, so that it can be written as $W(k)$. A consequence is that $W(k)$ is a Gaussian random variable with null mean and variance equal to $k\sigma^2$. In fact $\mu(W(k)) = k\mu(W(1)) = 0$, and $\sigma^2(W(k)) = k\sigma^2(W(1))$.

Note that saying that the increments are stationary, or that the increment process $W(k) = B(t)\text{-}B(t+k)$ is independent of *t* can also be expressed by saying that the Brownian motion is memoryless. At any instant $\bar{t}$ the evolution of the process for $t > \bar{t}$ is only dependent on the value $B(t)$, in particular it is independent of past history.

The same concepts can be applied to the continuous time domain, where $W(\tau) = B(t)\text{-}B(t+\tau)$ is the difference process, which is independent of *t*, but only depends on τ. As with the discrete case, $W(\tau)$ has a null mean and a variance proportional to τ. $B(t)$, in the continuous domain, can be viewed as the integral of white Gaussian noise, or even as the output of a linear system with a transfer function *G* such that $|G(f)|^2 \propto f^{-2}$ whose input is fed with white Gaussian noise. Hereafter, unless otherwise specified, we will refer to Brownian motion without distinguishing between discrete and continuous time.

Gaussian Brownian motion, as defined above, is a statistically self-affine process such that $B(t)$ is statistically indistinguishable from $\sqrt{r}B(t/r)$. This property will be central to the following discussions. It means that stretching the stochastic process $B(t)$ along the horizontal axis by *r* times and along the vertical axis by $\sqrt{r}$ times yields a new stochastic process which has the same statistics as $B(t)$ or, more precisely, $B(t)$ and $\sqrt{r}B(t/r)$ have the same finite dimensional joint distributions. The reason is that $B(t)$ is completely defined by the variance of the null-mean, Gaussian increments $W(\tau) = B(t)\text{-}B(t+\tau)$ and, since the variance of $W(\tau)$ is proportional to τ, $B(t)$ has increments that are distributed like those of $\sqrt{r}B(t/r)$. This fact can also be expressed by saying that the "slowed" process $B(t/r)$ is *properly rescaled* by magnifying it by $r^{0.5}$ times.

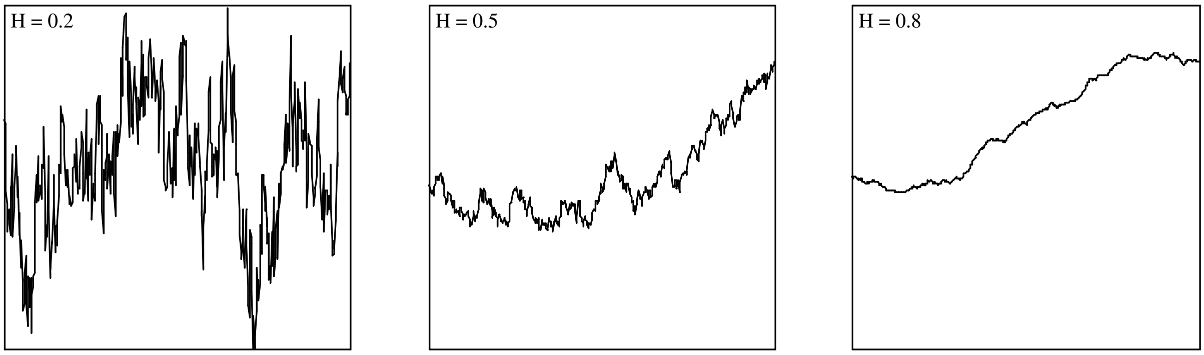

Figure 1: Fractional Brownian motion with three different values of the Hurst parameter.

Fractional Brownian motion (fBm) is an extension of these concepts. Gaussian fBm can be defined as a process with stationary Gaussian increments such that $B(t)$ has the same statistics as $r^H B(t/r)$, where $H \in [0; 1]$ is known as the *Hurst parameter* of the process. The same process can be obtained by filtering white Gaussian noise through a linear system with transfer function G such that $|G(f)|^2 \propto f^{-\beta}$, where $\beta = 1+2H$, hence $\beta \in [1; 3]$ [4, §1.4.2]. Figure 1 shows several instances of fBm processes with different values of the Hurst parameter. The increments of fBm are correlated, apart from the case H = 0.5, when fBm is reduced to "ordinary" Brownian motion, whose increments are uncorrelated.

The fractal dimension of the trace of one-dimensional fBm is $D = 2\text{-}H$ [4, §1.6], while the *zeroset* of an fBm trace, that is its intersection with the ordinate axis, has a dimension $D = 1\text{-}H$ [3, p. 252]. We call *zeroset gaps* the intervals of return of the trace to 0, that is, the distances between successive points in the zeroset. It can be shown that the lengths U of the gaps have a power (Pareto) distribution, such that $\mathrm{P}\{U > u\} = t^{-D}$ [3, p. 236]. A distribution of this kind has the effect of clustering the instants of crossing of a horizontal line, even though the gap lengths are independent. Looking at a zero at a higher level of detail, almost every zero is replaced by a whole cluster of points [3, p. 240].

The difference process of a Gaussian fBm is called Gaussian *Hurst noise* [3, pg.249], or fractional Gaussian noise (fGn for short). For $H = 0.5$, fGn is the ordinary white Gaussian noise, which exhibits no persistence, that is, its values at different points are uncorrelated. For $0.5 < H \leq 1$, fGn is *persistent* (positively autocorrelated), while it is *antipersistent* (negatively autocorrelated) for $0 \leq H < 0.5$. The power spectrum of fGn is proportional to $f^{-\beta+2}$.

fGn is observed in many natural and artificial phenomena: in most electronic components of varying degrees of complexity and different technologies, in time measurements, in the flow variations of rivers [3, p.249], in the flow of automobiles in expressways [8], and in that of packets in a local area network [7]. It is also found in both the pitch and loudness values of ancient and contemporary music in practically all cultures [4, §1.2.4].

We have said that fBm with $H > 0.5$ has positively correlated increments. This means that, once the trace begins to grow, it is more likely that it will continue to grow rather than decrease. The opposite is true when $H < 0.5$: after a positive increment, a negative increment is more likely. For ordinary Brownian motion, where $H = 0.5$, any increment is independent of the past history of the motion. The visual appearance of an fBm trace is increasingly jagged as H decreases from 1 to 0. In the border case of $H = 1$, the trace is a straight line whose slope is Gaussian, and whose fractal dimension is 1, equal to the topological dimension. In the other border case, $H = 0$, fBm becomes a kind of 1/f noise, the most common kind of noise found in nature whose origin, many decades of investigation notwithstanding, is still a mystery [4, §1.2.3]. Thus ordinary Gaussian Brownian motion is in the middle between a straight line and a Gaussian 1/f noise.

An fBm process is described by two parameters alone: its unitary variance $\sigma^2 = W(1)$ and its Hurst parameter H. Let us view fBm as the graph of the displacement of a fractional Gaussian random walker moving in discrete steps. σ represents the walker's speed, or the mean square root of the length of his/her steps. H represents the walker's tendency to follow the same direction after each step. When $H > 0.5$, the correlation between successive steps is positive, so the direction is usually the same. The correlation is negative if $H < 0.5$, so the direction is usually inverted at each step, and no correlation exists between successive steps when $H = 0.5$, that is, when the process is a memoryless ordinary Brownian motion.

4. Characterisation of the scintillation process

We started from a data set chosen from the results of the propagation experiment, in Ka band, carried out on the Olympus satellite by the CSTS (Centro Studi sulle Telecomunicazioni Spaziali) Institute, on behalf of the Italian Space Agency (ASI). The up-link (30 GHz) and down-link (20 GHz) samples considered were 1 second averages, expressed in dB, of the signal power attenuation with respect to clear sky conditions. The samples relate to 10 significant events for a total of 180,000 s recorded at the Spino d'Adda (North of Italy) station, collected from August to October, 1992. The slant path elevation angle was 30.6° and the antenna diameter was 3.5m.

The attenuation versus time plot recalls the behaviour of a self-similar or self-affine process (see Figure 1), whose analysis normally entails inspecting samples over a wide range of time scales. However, since our study focuses on fade countermeasure systems, we only look at the characteristics of the process in the range of a few seconds (this choice will be discussed later on), instead of considering the overall shape of the trace of the attenuation events. In practice, we analyse the scintillation process, which is commonly identified for frequencies above a few hundredths of a Hertz (0.02-0.03 Hz in [1, 20]). We expect to find that the scintillation process depends on the rain fade level, other conditions being equal. In other words, we are trying to find a dependence of the high-frequency component of the attenuation process (i.e. scintillation) on the low-frequency component of the same process (i.e. rain fade). To this end, we analyse the difference process of the scintillation using the following procedure.

Denoting by A the attenuation value expressed in dB, we consider the difference process $W(t_1,t_2)=A(t_2)-A(t_1)$ which, for sufficiently small $t=t_2-t_1$, is the difference process of the scintillation. Under the same assumption of a sufficiently small t, we assume that the scintillation process is stationary. In order to investigate the behaviour of the scintillation process versus the rain fade level, we divide the entire sample data into rain fade bins, with an amplitude of 1 dB for the down- and 2 dB for the up-link rain fades, respectively. Thus, denoting by A_n the rain fade at the centre of the n-th bin, we have $W(t_1,t_2,A_n)=W(t,A_n)$ for t << 1/0.03, according to the above cited figures. In order to find the rain fade level relative to each sample, we use a sharp low-pass filter with a cutoff frequency of 0.1 Hz.

The available data are samples of the attenuation process averaged over 1 s intervals, i.e. we only have $A(t)$ with t = 1, 2, 3, …. For each pair of values t and A_n, the process W is assumed to have the distribution $N(0,\ \sigma_W^2)$. Indeed, a Chi-Square test on the distribution of $W(t, A_n)$ gives acceptable results for values of t = 1, 2 and 3 s, i.e. in the order of 1-5% level of significance. We notice that a related assumption is made in [20, 23, 28], where the variance of the scintillation is considered. Unfortunately, while the lower bins are very rich in samples, the higher ones are not, because of the low probability of recording very high attenuation values. In these cases the above assumption is not proved by our data, so we limited our analysis to the attenuation range where an acceptable number of samples is available for each bin. Fixing this number to 300, the attenuation limits are 25 dB for the up-link and 16 dB for the down-link, respectively.

By visual inspection and by analogy with many natural phenomena, as previously discussed, we approximate the scintillation with an fBm process. We begin by computing the Hurst parameter of the scintillation process, then we show a visual justification of our hypothesis.

We assume that the variance of the scintillation difference process W can be expressed as

$$\sigma_W^2 = Vt^{2H}, \tag{1}$$

where the parameters H (the Hurst parameter) and V generally depend on A_n.

To evaluate such parameters, $\sigma_W^2(t,A_n)$ is computed for A_n from A_1 to $A_{n_{\max}}$ dB, and for t equal to 1, 2 and 3 s. For each value τ of t, $\sigma_W^2(\tau,A_n)$ is the variance of $W(\tau,A_n)$, that is, the variance of $[A(\bar{t}+\tau)-A(\bar{t})]$, for all $\bar{t}$ such that the low-frequency component of $A(\bar{t})$ belongs to the bin A_n. Then, for each value τ of t, the values of $\sigma_W^2(\tau,A_n)$ are interpolated with a 3rd order polynomial to smooth the data (see Figure 2a). Finally, for each A_n, equation (1) is used to fit the smoothed data using a non-linear least square interpolation method with parameters V and H (see Figure 2b).

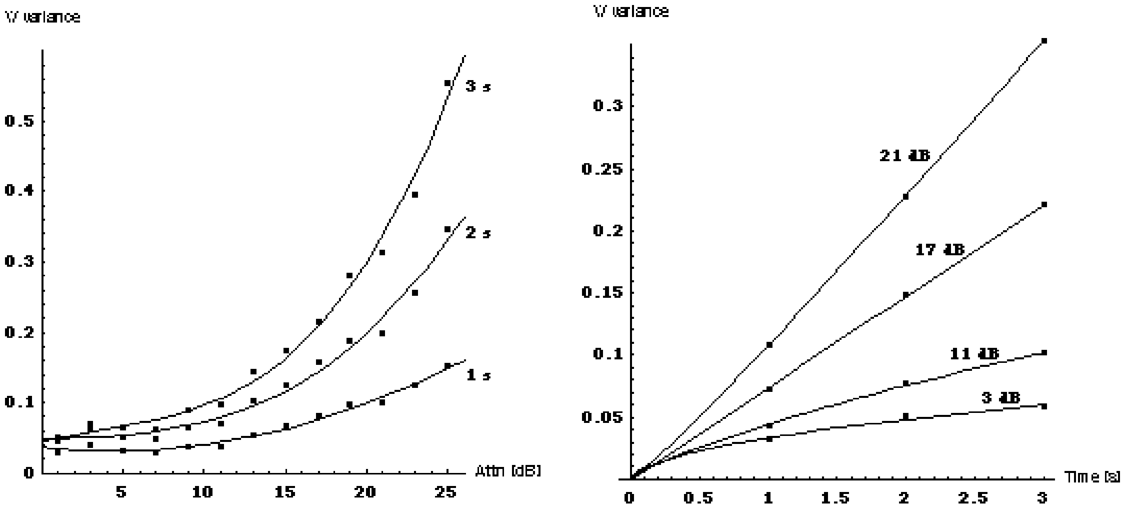

(a) (b)

Figure 2: Examples of data interpolations: a) smoothing the original data. b) fitting equation (1) to the smoothed data.

The resulting values for the V and H parameters in the up-link (V_u, H_u) and in the down-link (V_d, H_d) are plotted in Figure 3 versus the rain fade A_n. The following interpolating polynomials of V and H are also depicted:

$$\begin{cases} V_u = 0.033 + 9.4 \cdot 10^{-5} A_u + 9.7 \cdot 10^{-6} A_u^2 + 7.5 \cdot 10^{-6} A_u^3 \\ V_d = 0.02 - 0.0022 \ A_d + 0.00035 \ A_d^2 \end{cases}, \qquad \begin{cases} H_u = 0.23 + 0.014 A_u \\ H_d = 0.23 + 0.019 A_d \end{cases}.$$

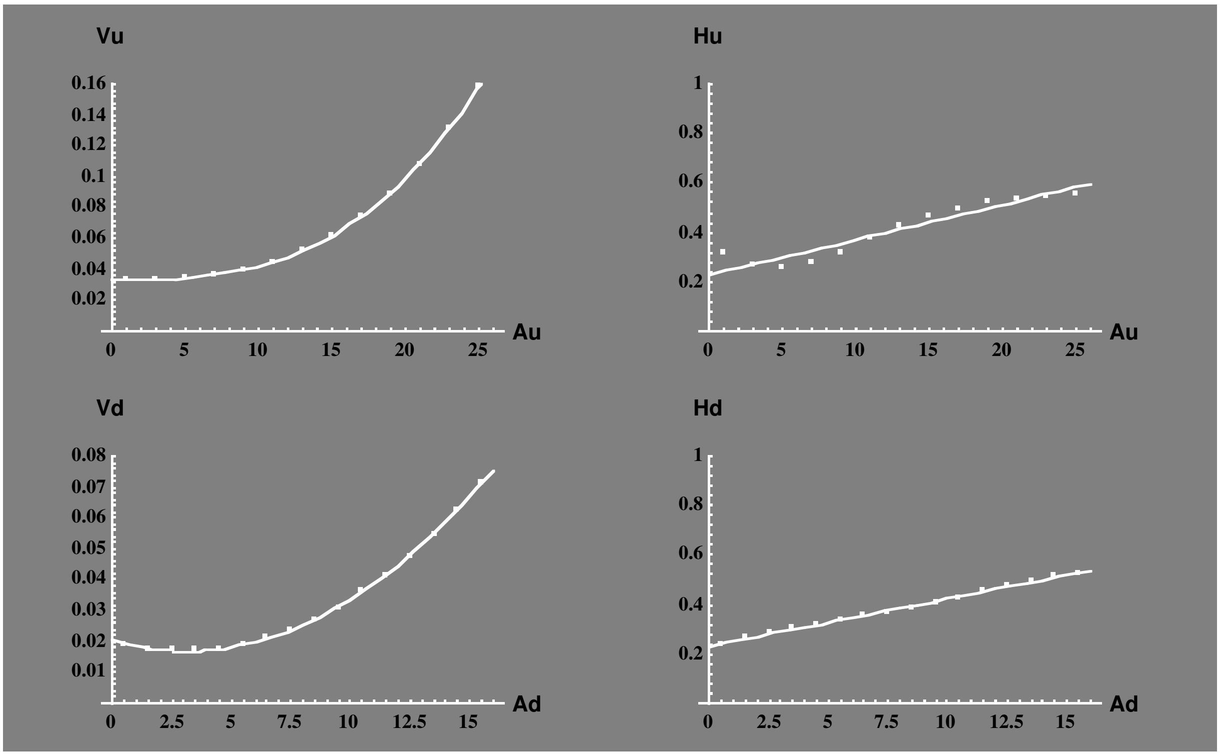

Figure 3: Interpolation of the parameters V and H as functions of up and down-link attenuations

The method followed does not rigorously give an indication as to the self-affine nature of the process, nor does it give a precise estimation of the Hurst parameter. Other methods are commonly used to estimate the Hurst parameter of a process [6, 7], one of which can be used to compute confidence intervals. All these methods also give an idea of whether the process being measured can be considered to be self-affine. In order to get such information, an analysis of the process that spans several decades of time scales is required, while we only focused on the very limited range 1-3 s. One reason for this choice, as already mentioned, is that we are not interested in longer time spans, because our aim is to study fade countermeasure systems. More importantly, extending the time range is not possible, because of the influence of the rain fade process at lower frequencies. In other words, the hypothesis of a stationary scintillation process does not hold for time ranges greater than a few seconds. This is not really a problem for our purposes, since we are trying to characterise the short-term behaviour of the scintillation process in order to find the dependencies of its parameters on the attenuation.

Given the above observations, it would be more precise to use the term *pseudo-Hurst parameter* when dealing with the value of *H* obtained with the described method. However, for simplicity's sake, we'll continue to call *H* the Hurst parameter.

In order to get a visual impression of the self-affine property, Figure 4 plots different portions of the attenuation, each rescaled using the computed Hurst parameter.

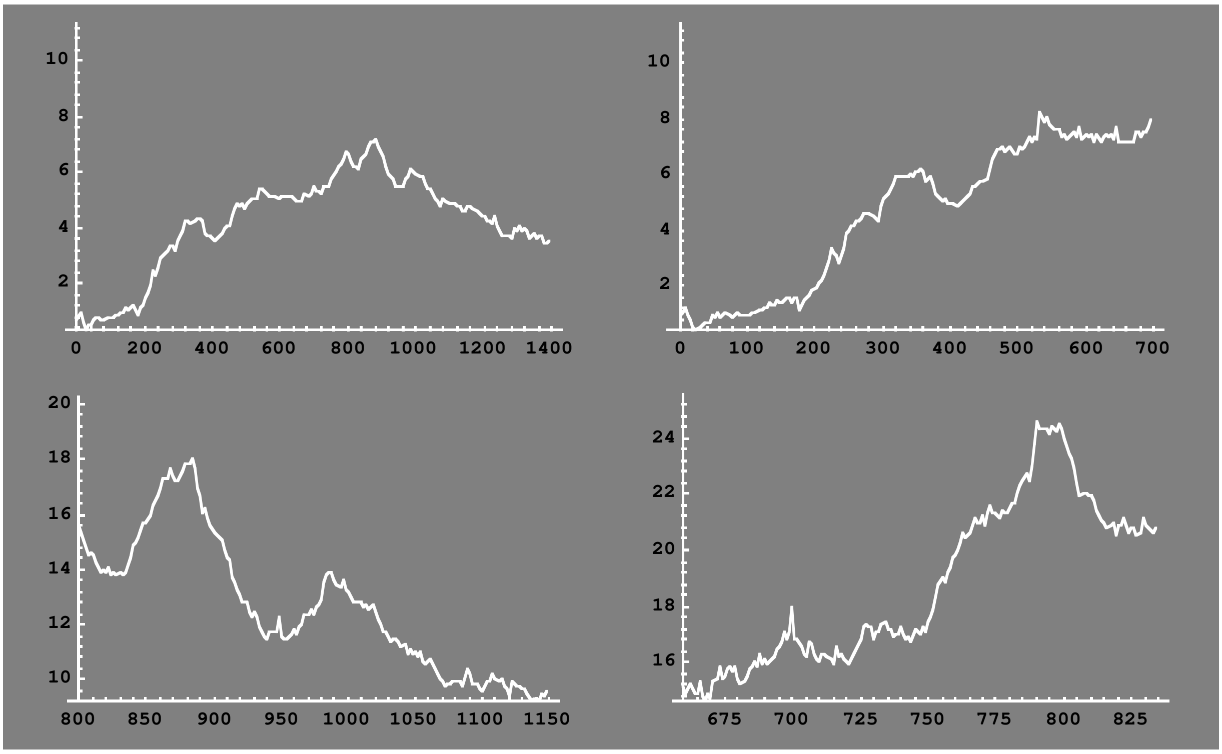

Figure 4: Rescaled portions of the attenuation time sequence. The numbers on the horizontal axis are seconds, those on the vertical axis are rescaled dB.

5. Physical considerations about fractal characterisation

The interpolation criterion we have described so far is based solely on geometrical considerations. Indeed, all parameters are deduced from an analysis of the values of the measured samples. Let us try to support this procedure which some justification that builds on physical findings and theories. In this section we suggest some possible explanations and analogies, most of which should be taken as ideas for further research in this potentially fertile field.

The fundamental relationships we found are that the scintillation power σ^2 and its Hurst parameter are both dependent on the attenuation. As far as the scintillation power is concerned, most authors would admit that it should be considered constant with respect to the attenuation value. However, recent findings [20] suggest that a relationship exists, and it has the same sign as our statistics show.

Preprint of an article published on the IEEE JOURNAL on SELECTED AREAS in COMMUNICATIONS, VOL. 17, No. 2

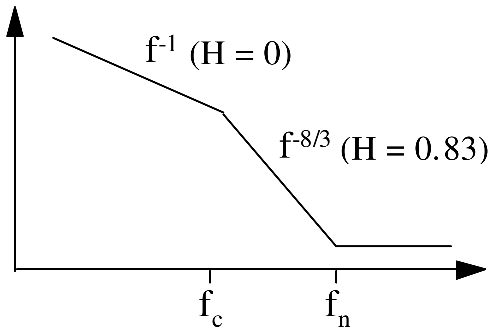

Figure 5: Power spectrum of the scintillation process as described in [1].

As far as the variability of the parameter H with the attenuation value is concerned, we will refer to the spectral analysis of the scintillation process. In fact, it is commonly accepted [1, 20, 22] that the power spectrum of the scintillation in log-log scale follows an f^{-1} slope followed by an $f^{-8/3}$ slope, as shown in Figure 5, and that the corner frequency f_c is dependent on many parameters. The high frequency part of the scintillation spectrum when rain occurs, is similar to that observed in clear sky conditions [28]. To our knowledge, no studies exist on the dependence of the corner frequency upon the attenuation value. In any case, f_c is usually assumed to lie in the range 0.04-0.66 Hz, which is compatible with the time range 1-3 s of our analysis. If f_c lies within this range, then its dependence on the rain fade, whose laws are as yet unknown, can be reasonably thought to cause the dependence of the Hurst parameter on the rain fade. In fact, as outlined above, the power density spectrum of an fBm process exhibits a slope of $f^{-\beta}$, where $\beta = 1{+}2H$. Since we assume that the slopes of the power density spectrum of the scintillation process around f_c are f^{-1} for $f < f_c$ and $f^{-8/3}$ for $f > f_c$, H should lie in the range [0; 0.83]. This observation is significant because this range is compatible both with the permitted range of H, which is [0; 1], and with our findings, which give a range of approximately [0.2; 0.6]. Here we suggest that the dependence we observed of the Hurst parameter on the attenuation can be attributed to the variability of the scintillation power spectrum with the rain fade. If the spectrum is approximated by two asymptotes with slopes f^{-1} and $f^{-8/3}$, then H can be thought of as a function of f_c, which in turn depends on the rain fade.

In order to obtain this function, while finding further confirmation of our hypothesis, we analysed a numerically generated scintillation noise, taking the model depicted in Figure 5 as the power spectrum. We set f_n equal to 3 Hz, using the value measured in [20], and we measured the pseudo-Hurst parameter of the resulting process versus f_c. The result of the experiment is plotted in Figure 6. The process was generated with a frequency of 64 Hz and then integrated and dumped in 1 s intervals, thus simulating the measurement procedure of the attenuation samples at our disposal. The H parameter was measured in the time span of 3 s. It was interesting to notice how using a frequency higher than 1 Hz for the integrate and dump procedure didn't produce significative changes in the results while in the range [1, 8] Hz. For higher frequencies our method for measuring the pseudo-Hurst parameter began giving inconsistent results, because of the background noise above 3 Hz. The same background noise is the reason why the samples in the plot deviate from a straight line for f_c greater than approximately 0.3 Hz.

In order to keep the analysis simple, we adopted a first-order least squares fit to the first 65 samples, covering a frequency range for f_c equal to [0.04, 0.25] Hz, thus obtaining $H = 0.83 - 1.7 f_c$. This equation coupled with the interpolating functions (1) let us obtain the following tentative relationships between f_c and the atmospheric attenuation A expressed in dB:

$$f_c = 0.35 - 0.008 A_u, \quad f_c = 0.35 - 0.011 A_d.$$

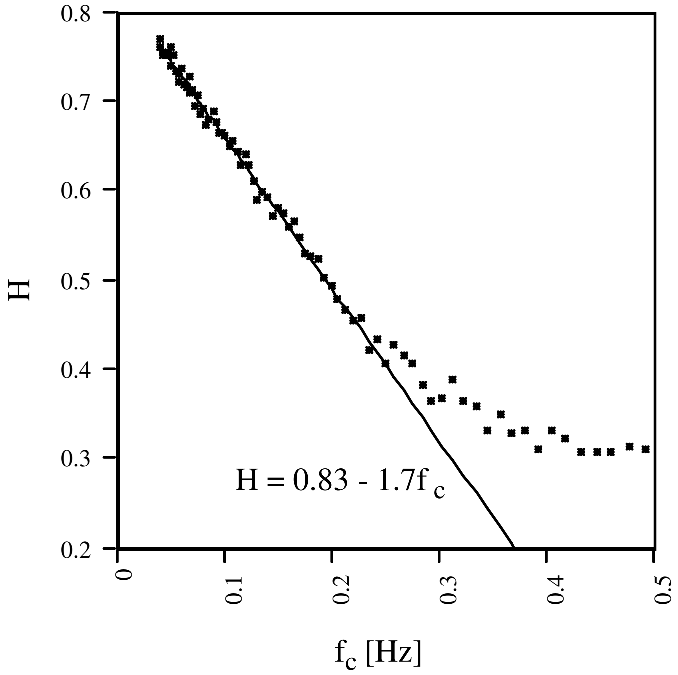

Figure 6: Results of the numerical experiment of measuring the pseudo-Hurst parameter of a synthetically generated scintillation noise while varying f_c.

As a consistency check of the overall procedure, we applied it to simulated samples with f_n set to infinity, and setting f_c either to 0 or to infinity, thus obtaining a power spectrum with a single slope of either -1 or -8/3. As expected, we were able to make precise measurements of the Hurst parameter, by considering intervals of time significantly longer than 3 s. The same measurements made in the presence of more than one slope in the power spectrum yields inconsistent results for long time intervals, analogously to the real samples.

Preprint of an article published on the IEEE JOURNAL on SELECTED AREAS in COMMUNICATIONS, VOL. 17, No. 2

The modeling of scintillation as an fBm process (at least for the time scales mentioned) makes even more sense when the distribution of the zeroset gap lengths is analysed. As mentioned above, we would expect this distribution to decay like u^{-D}, where $D = 1\text{-}H$, that is, D should lie in the range [0.17; 1]. From [27], in fact, we can see that, at least in the frequency range [0.3; 3] Hz, which is the significant range for our analysis, the slope of the measured distribution is compatible with our model.

6. Random midpoint displacement interpolation

Once we assume that the scintillation process is fractal, and that it can be described locally as an fBm whose parameters are functions of the local attenuation value, we can finally use a meaningful method to interpolate the process between successive samples. Our assumption is that the fractal characterisation of the scintillation process we have made in the time range 1-3 s also holds for smaller time scales. The scintillation at smaller time scales can then be approximated in a significant way by an fBm process whose fractal dimension is locally that of the scintillation process, which we know from the previous procedure.

We then need to synthesise a pseudo-random fBm process with the constraints that its graph passes through the 1 s samples of the measured attenuation, and that its σ^2 and its fractal dimension (hence the Hurst parameter) are locally the same as those of the measured attenuation.

Of the various methods available for generating fBm, many of which are dealt with in [3, 4], we chose the random midpoint displacement algorithm, rmd for short [6]. It is much simpler and quicker than the other methods, though it is only an approximation of a real fBm process. Despite this, rmd is sufficient for most uses. In [6] the authors show that an acceptable degree of precision is achieved as far as the target value of H is concerned, unless H is very far from the central value 0.5. For the kind of application we are investigating the interesting values of the Hurst parameter are generally close to 0.5, which makes rmd acceptable for our purposes. The authors of [6] also suggest that rmd is particularly suitable for fractal interpolation, as this application only minimally suffers from the imperfect correlation between different points in the synthetic trace. In fact, the overall behaviour of the trace is dictated by the samples that are interpolated.

An example of random fractal interpolation obtained using rmd is given in Figure 7. Here, 14 samples of measured attenuation at 30 Ghz are interpolated in order to get 50 samples per second, instead of the original 1 sample per second. The values of H and of the standard deviation of random generated samples are computed from the model that is described above. The graph in Figure 7 is only an example of the infinite number of ways to randomly interpolate some given points, all of which share the same statistical parameters.

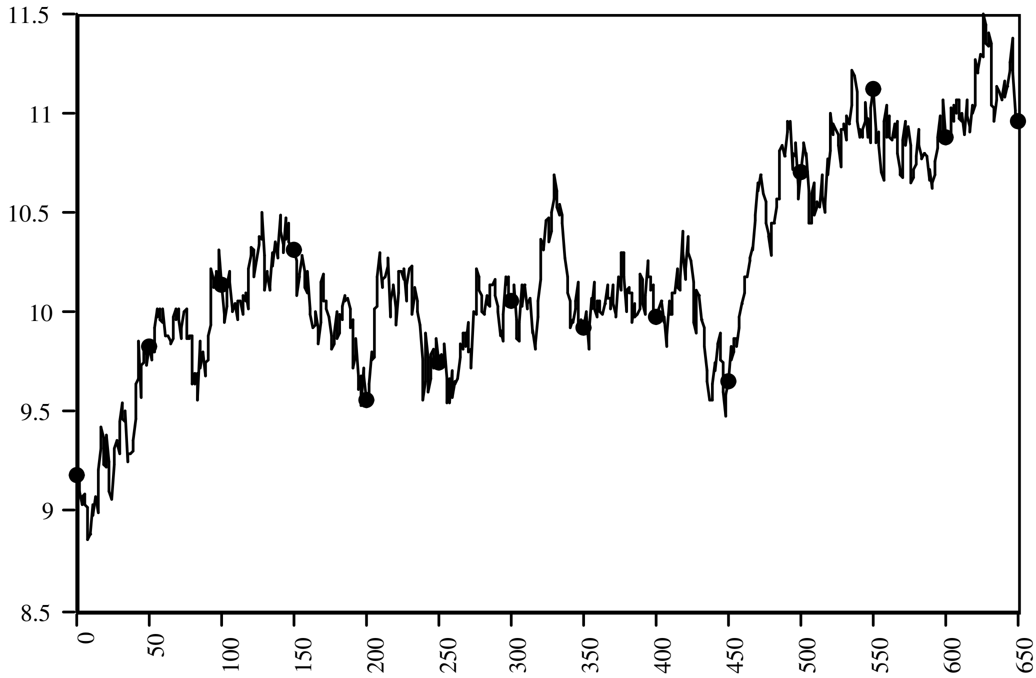

Figure 7: An example of the interpolation procedure. Starting from 14 1 s-spaced points we randomly compute 50 values per second. Values on the horizontal axis are 1/50-th of a second, values on the vertical axis are attenuations in dB.

7. Optimising measurement times for fading estimation.

The methods to estimate the signal degradation reported in [14-16, 26] are based on measurements made either on the bit error rate or on pseudo-error statistics. The hard or soft decision levels of the demodulated data bits are inspected to obtain a measure of signal quality, usually the value of E_b/N_o. The estimation obtained has a variance which is inversely proportional to the number of inspected bits and thus to the measurement time interval. Considering that the variance of the attenuation increases with time according to our model, expressed by relation (1), it is possible to optimise the measurement times [26].

Let us denote by t_Δ the interval of time between the estimation of the signal degradation and the instant the destination user receives data sent with the adaptive countermeasure chosen according to the estimation. Let t_m be the measurement time, and let us assume that the measurement error and the attenuation difference process are independent and both Gaussian. The total error on the signal quality estimation is then Gaussian with a variance σ_q^2 given by

$$\sigma_q^2 = \sigma_m^2(t_m) + \sigma_\Delta^2(t_m + t_\Delta)$$

where σ_m^2 is the variance of the measurement error and σ_Δ^2 is the variance of signal quality evolution at the time $t_m + t_\Delta$, computed according to our attenuation model. t_Δ depends on the fade countermeasure system adopted, and can be assumed to be constant. σ_m^2 decreases, while σ_Δ^2 increases with the measurement time, and σ_q^2 can be minimised with respect to t_m. Once the minimum σ_q^2 has been obtained, a suitable power margin can be computed in order to guarantee the bit error rate (BER) required by the user. The margin M, which is generally dependent on the characteristic of the BER versus the signal to noise ratio, and thus dependent on the modulation/coding scheme, is computed as follows.

Denoting by p_e the probability of error, and by R the channel E_b / N_0 (bit energy over the one sided noise spectral density) expressed in dB, we assume that we know the relation $p_e(R)$ at the data decoder for the coding type considered. The average p_e, for a given value $\overline{R}$ of the channel E_b / N_0, which is estimated with a variance $\sigma_{\overline{R}}^2$, is given by

$$p_e(\overline{R}) = \int_{-\infty}^{+\infty} p_e(R) \frac{1}{\sqrt{2\pi}\ \sigma_{\overline{R}}} e^{-\frac{(R-\overline{R})^2}{2\sigma_{\overline{R}}^2}} dR \qquad (2)$$

Substituting p_e given by (2) in the inverse function of $p_e(R)$, we get the equivalent value $R_e\left(p_e(\overline{R})\right)$. The margin to be applied on the estimated value $\overline{R}$ is then $M(R) = \overline{R} - R_e$.

For a numerical example, we have considered B/QPSK modulated data, both uncoded and convolutionally encoded (k = 7, rate =1/2) and Viterbi decoded. For the uncoded case we have [24]

$$p_e = \frac{1}{2} erfc\left(10^{R/20}\right). \qquad (3)$$

For the 1/2 coded case, by interpolating the decoder results [25], we have obtained the function

$$p_e = 10^{-(1.6R+3)}, \qquad (4)$$

which is linear in bilogarithmic scale. For the evaluation of the integral in (2) it is sufficient to consider the integration limits of $\pm 3\sigma_R$ to get a good approximation. This assures us about the validity of the application field of relations (3) and (4).

In Figure 8 the margin M is reported as a function of the variance σ_R^2, and, in the uncoded case, for various values of E_b / N_0. Since M increases with the absolute value of the derivative of the function $p_e(R)$, there is no dependence on E_b / N_0 in the 1/2 coded case, where this derivative is constant.

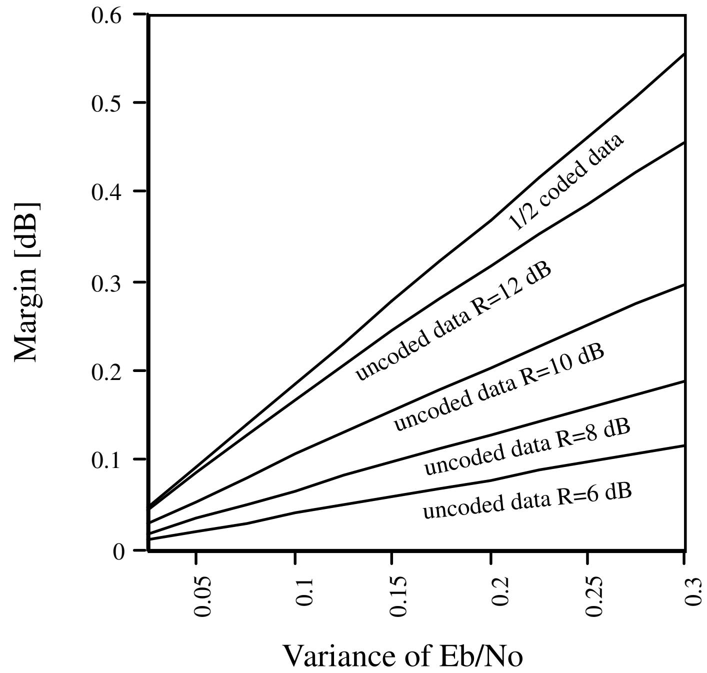

Figure 8: Margin to take into account over the estimation of the E_b / N_0 *ratio as functions of the* E_b / N_0 *variance. Both uncoded and 1/2 coded cases are shown.*

Conclusions

The model we have presented characterises the short time evolution of the attenuation process, mostly due to scintillation, which is assumed to be stationary when the rain fade stays the same.

We have considered attenuation sample data, spread over a two-month period, at two fixed frequencies, and with a fixed elevation angle and antenna size, so no attempt has been made to consider the dependency of the process on these factors. It is well known [21] that the amplitude of rapid level fluctuations of the attenuation depends on a lot of factors such as elevation angle, antenna gain, season and latitude of the earth station. Corrections to apply for different elevation angles and antenna sizes can be found in [22], while [23, 28] gives some ideas about the dependence on season and on some other factors in clear air conditions alone. We conclude therefore that the derivation of a model which has a more general validity needs a more thorough statistical analysis and a much larger sample of attenuation data.

The model presented should be viewed as a proposal for further investigations. Should it prove to be reliable, it would be useful for the study of fade countermeasure systems such as those required in digital satellite communications, especially when the Ka band is employed.

Preprint of an article published on the IEEE JOURNAL on SELECTED AREAS in COMMUNICATIONS, VOL. 17, No. 2

Acknowledgements

The authors wish to thank Dr. Mario Mauri from the CSTS (Centro Studi sulle Telecomunicazioni Spaziali) Institute for his collaboration.

References

[1] Y.Karasawa, T.Matsudo, “Characteristics of fading on low-elevation angle earth-space paths with concurrent rain fade and scintillation”, IEEE Transactions on antennas and propagation, vol.39, no.5, May 1991.

[2] N. Celandroni, E. Ferro, N. James and F. Potortì, “FODA/IBEA: a flexible fade countermeasure system in user oriented networks,”Intern. Journal of Satellite Communications, Vol. 10, No. 6, pp. 309-323, 1992.

[3] Benoit B. Mandelbrot, “The fractal geometry of nature”, Freeman & Co., New York, 1983.

[4] Heinz-Otto Peitgen, Dietmar Saupe “The science of fractal images”, Springer-Verlag, 1988.

[5] L. Dossi E. matricciani and M. Mauri, “Robust control system for resource-shared satellite networks affected by rain fade” Alta Frequenza vol. 6 n. 6 Nov-Dec. 1994.

[6] Lau, Erramilli, Wang, Willinger, “Self-similar traffic generation: the random midpoint displacement algorithm and its properties”, Int. Conf. on Communications, June 1995, Seattle, USA, 466-472.

[7] W. E. Leland, M. S. Taqqu, W. Willinger and D. V. Wilson, “On the self-similar nature of Ethernet Traffic (extended version),” IEEE/ACM Transactions on Networking, Vol. 2, No. 1, February 1994.

[8] Musha, Higuchi, “The 1/f fluctuation of a traffic current on an expressway”, Jap. J. Appl. Phys. 15, 1976, 1271-1275.

[9] H. Kazama, T. Atsugi, M. Umehira and S. Kato, “A Feedback-Loop Type Transmission Power Control for Low Speed TDMA Satellite Communication Systems,” Proc.IEEE ICC ’89, Boston MA.

[10] E. Russo, “Implementation of a space diversity system for Ka-band satellite communications,”IEEE ICC 1993.

[11] CCIR Report 564-4, “Propagation data and prediction methods required for earth- space telecommunications systems,” 1990.

[12] L. Dossi, G. Tartara and E. Matricciani, “Frequency diversity in millimeter wave satellite communications, ”IEEE Trans. on Aerospace and Electronic Systems vol.28,n.2, April 1992.

[13] F. Carassa, E. Matricciani and G. Tartara, “Frequency diversity and its applications,” International Journal of Satellite Communications, vol. 6, pp.313-322 (1988).

[14] N. Celandroni, "Estimation of the Eb/No ratio using PSK quantised levels in an additive white Gaussian noise (AWGN) environment," CNUCE Report C90-22, September 1990.

[15] D. Kreuer and E.Bierbaum "Improved Eb/No Estimation with Soft Quantized Detection," Proc.PIMRC'94/WCN, Den Haag, The Netherlands, Sept. 1994, pp. 620-624.

[16] N. Celandroni, E. Ferro and F. Potortì, "Quality estimation of PSK modulated signals", IEEE Communications Magazine, vol 35, n.7, July 1997.

[17] J. S. Bendat and A. G. Piersol," Random Data: Analysis and Measurement Procedures". Wiley and Sons, 1986.

[18] Peitgen, Jurgens and Saupe, "Chaos and Fractals", Springer-Verlag, New York 1992.

[19] M. Barnsley, "Fractals everywhere", chapter 6: Fractal interpolation. Academic press Inc., 1988.

[20] E. Matricciani,M. Mauri, C. Riva, "Relationship between scintillation and rain fade at 19.77 GHz", Radio Science, Vol.31, No.2, 273-279, March-April 1996.

[21] M. Filip and E. Vilar, "Optimum utilization of the channel capacity of a satellite link in the presence of amplitude scintillations and rain fade" IEEE Trans. on Comm. vol. 38 n. 11, November 1990.

[22] Vilar, Filip, "Measurements of 20-30 Ghz amplitude scintillations. Dependence of the statistics upon the ground station measuring parameters", Proc. Olympus utilisation conference, Vienna, 1989.

[23] G. Peeters, F. S. Marzano, G. D'Auria, C. Riva, D. Vanhoenacker-Janvier, "Evaluation of statistical models for clear-air scintillation prediction using Olympus satellite measurements", Int. J. Satellite Comm., Vol.15, 1997, 73-88.

[24] J. G. Proakis, Digital Communications. McGraw-Hill, 1995.

[25] N. Celandroni, E. Ferro, N. James and F. Potortì, "FODA/IBEA: a flexible fade countermeasure system in user oriented networks," Intern. Journal of Satellite Communications, Vol. 10, No. 6, pp. 309-323, 1992.

[26] N. Celandroni and S. T. Rizzo, "Detection of Errors Recovered by Decoders for Signal Quality Estimation on Rain Faded AWGN Satellite Channels", IEEE Transactions on Communications, Vol. 46 n.4, pp. 446-449, 1998.

[27] O.P.Banjo, E.Vilar, "Dynamic characteristics od scintillation fading on a low elevation earth-space path", Proc. URSI wave propagation: remote sensing and communications, Durham NH USA, 1986.

[28] D. Vanhoenacker, G. Brussard, F. Haidara, G. Ortgies, A. Paraboni, T. Pratt, C. Riva, J. Tervonen, S. Touw, H. Vasseur, " Atmospheric scintillation", OPEX 2nd Workshop of the Olympus Propagation Experiments, ESA/ESTEC, Noordwijk (NL), ESA WPP-083, Vol. 2 Chapter V, pp. 50-65, November 1994.